

This is the accepted manuscript made available via CHORUS. The article has been published as:

Bounds on an Anomalous Dijet Resonance in W+jets Production in pp[over ^] Collisions at sqrt[s]=1.96 TeV

V. M. Abazov *et al.* (D0 Collaboration)

Phys. Rev. Lett. **107**, 011804 — Published 30 June 2011

DOI: [10.1103/PhysRevLett.107.011804](https://doi.org/10.1103/PhysRevLett.107.011804)

Bounds on an anomalous dijet resonance in $W +$ jets production in $p\bar{p}$ collisions at $\sqrt{s} = 1.96$ TeV

V.M. Abazov,³⁵ B. Abbott,⁷³ B.S. Acharya,²⁹ M. Adams,⁴⁹ T. Adams,⁴⁷ G.D. Alexeev,³⁵ G. Alkhazov,³⁹ A. Alton,^{a,61} G. Alverson,⁶⁰ G.A. Alves,² M. Aoki,⁴⁸ M. Arov,⁵⁸ A. Askew,⁴⁷ B. Åsman,⁴¹ O. Atramentov,⁶⁵ C. Avila,⁸ J. BackusMayes,⁸⁰ F. Badaud,¹³ L. Bagby,⁴⁸ B. Baldin,⁴⁸ D.V. Bandurin,⁴⁷ S. Banerjee,²⁹ E. Barberis,⁶⁰ P. Baringer,⁵⁶ J. Barreto,³ J.F. Bartlett,⁴⁸ U. Bassler,¹⁸ V. Bazterra,⁴⁹ S. Beale,⁶ A. Bean,⁵⁶ M. Begalli,³ M. Begel,⁷¹ C. Belanger-Champagne,⁴¹ L. Bellantoni,⁴⁸ S.B. Beri,²⁷ G. Bernardi,¹⁷ R. Bernhard,²² I. Bertram,⁴² M. Besançon,¹⁸ R. Beuselinck,⁴³ V.A. Bezzubov,³⁸ P.C. Bhat,⁴⁸ V. Bhatnagar,²⁷ G. Blazey,⁵⁰ S. Blessing,⁴⁷ K. Bloom,⁶⁴ A. Boehnlein,⁴⁸ D. Boline,⁷⁰ E.E. Boos,³⁷ G. Borissov,⁴² T. Bose,⁵⁹ A. Brandt,⁷⁶ O. Brandt,²³ R. Brock,⁶² G. Brooijmans,⁶⁸ A. Bross,⁴⁸ D. Brown,¹⁷ J. Brown,¹⁷ X.B. Bu,⁴⁸ M. Buehler,⁷⁹ V. Buescher,²⁴ V. Bunichev,³⁷ S. Burdin^{b,42} T.H. Burnett,⁸⁰ C.P. Buszello,⁴¹ B. Calpas,¹⁵ E. Camacho-Pérez,³² M.A. Carrasco-Lizarraga,⁵⁶ B.C.K. Casey,⁴⁸ H. Castilla-Valdez,³² S. Chakrabarti,⁷⁰ D. Chakraborty,⁵⁰ K.M. Chan,⁵⁴ A. Chandra,⁷⁸ G. Chen,⁵⁶ S. Chevalier-Théry,¹⁸ D.K. Cho,⁷⁵ S.W. Cho,³¹ S. Choi,³¹ B. Choudhary,²⁸ S. Cihangir,⁴⁸ D. Claes,⁶⁴ J. Clutter,⁵⁶ M. Cooke,⁴⁸ W.E. Cooper,⁴⁸ M. Corcoran,⁷⁸ F. Couderc,¹⁸ M.-C. Cousinou,¹⁵ A. Croc,¹⁸ D. Cutts,⁷⁵ A. Das,⁴⁵ G. Davies,⁴³ K. De,⁷⁶ S.J. de Jong,³⁴ E. De La Cruz-Burelo,³² F. Déliot,¹⁸ M. Demarteau,⁴⁸ R. Demina,⁶⁹ D. Denisov,⁴⁸ S.P. Denisov,³⁸ S. Desai,⁴⁸ C. Deterre,¹⁸ K. DeVaughan,⁶⁴ H.T. Diehl,⁴⁸ M. Diesburg,⁴⁸ P.F. Ding,⁴⁴ A. Dominguez,⁶⁴ T. Dorland,⁸⁰ A. Dubey,²⁸ L.V. Dudko,³⁷ D. Duggan,⁶⁵ A. Duperrin,¹⁵ S. Dutt,²⁷ A. Dyshkant,⁵⁰ M. Eads,⁶⁴ D. Edmunds,⁶² J. Ellison,⁴⁶ V.D. Elvira,⁴⁸ Y. Enari,¹⁷ H. Evans,⁵² A. Evdokimov,⁷¹ V.N. Evdokimov,³⁸ G. Facini,⁶⁰ T. Ferbel,⁶⁹ F. Fiedler,²⁴ F. Filthaut,³⁴ W. Fisher,⁶² H.E. Fisk,⁴⁸ M. Fortner,⁵⁰ H. Fox,⁴² S. Fuess,⁴⁸ A. Garcia-Bellido,⁶⁹ V. Gavrilov,³⁶ P. Gay,¹³ W. Geng,^{15,62} D. Gerbaudo,⁶⁶ C.E. Gerber,⁴⁹ Y. Gershtein,⁶⁵ G. Ginther,^{48,69} G. Golovanov,³⁵ A. Goussiou,⁸⁰ P.D. Grannis,⁷⁰ S. Greder,¹⁹ H. Greenlee,⁴⁸ Z.D. Greenwood,⁵⁸ E.M. Gregores,⁴ G. Grenier,²⁰ Ph. Gris,¹³ J.-F. Grivaz,¹⁶ A. Grohsjean,¹⁸ S. Grünendahl,⁴⁸ M.W. Grünewald,³⁰ T. Guillemin,¹⁶ F. Guo,⁷⁰ G. Gutierrez,⁴⁸ P. Gutierrez,⁷³ A. Haas,^{c,68} S. Hagopian,⁴⁷ J. Haley,⁶⁰ L. Han,⁷ K. Harder,⁴⁴ A. Harel,⁶⁹ J.M. Hauptman,⁵⁵ J. Hays,⁴³ T. Head,⁴⁴ T. Hebbeker,²¹ D. Hedin,⁵⁰ H. Hegab,⁷⁴ A.P. Heinson,⁴⁶ U. Heintz,⁷⁵ C. Hensel,²³ I. Heredia-De La Cruz,³² K. Herner,⁶¹ G. Hesketh,^{d,44} M.D. Hildreth,⁵⁴ R. Hirosky,⁷⁹ T. Hoang,⁴⁷ J.D. Hobbs,⁷⁰ B. Hoeneisen,¹² M. Hohlfeld,²⁴ Z. Hubacek,^{10,18} N. Huske,¹⁷ V. Hynek,¹⁰ I. Iashvili,⁶⁷ Y. Ilchenko,⁷⁷ R. Illingworth,⁴⁸ A.S. Ito,⁴⁸ S. Jabeen,⁷⁵ M. Jaffré,¹⁶ D. Jamin,¹⁵ A. Jayasinghe,⁷³ R. Jesik,⁴³ K. Johns,⁴⁵ M. Johnson,⁴⁸ D. Johnston,⁶⁴ A. Jonckheere,⁴⁸ P. Jonsson,⁴³ J. Joshi,²⁷ A.W. Jung,⁴⁸ A. Juste,⁴⁰ K. Kaadze,⁵⁷ E. Kajfasz,¹⁵ D. Karmanov,³⁷ P.A. Kasper,⁴⁸ I. Katsanos,⁶⁴ R. Kehoe,⁷⁷ S. Kermiche,¹⁵ N. Khalatyan,⁴⁸ A. Khanov,⁷⁴ A. Kharchilava,⁶⁷ Y.N. Kharzeev,³⁵ M.H. Kirby,⁵¹ J.M. Kohli,²⁷ A.V. Kozelov,³⁸ J. Kraus,⁶² S. Kulikov,³⁸ A. Kumar,⁶⁷ A. Kupco,¹¹ T. Kurča,²⁰ V.A. Kuzmin,³⁷ J. Kvita,⁹ S. Lammers,⁵² G. Landsberg,⁷⁵ P. Lebrun,²⁰ H.S. Lee,³¹ S.W. Lee,⁵⁵ W.M. Lee,⁴⁸ J. Lelloch,¹⁷ L. Li,⁴⁶ Q.Z. Li,⁴⁸ S.M. Lietti,⁵ J.K. Lim,³¹ D. Lincoln,⁴⁸ J. Linnemann,⁶² V.V. Lipaev,³⁸ R. Lipton,⁴⁸ Y. Liu,⁷ Z. Liu,⁶ A. Lobodenko,³⁹ M. Lokajicek,¹¹ R. Lopes de Sa,⁷⁰ H.J. Lubatti,⁸⁰ R. Luna-Garcia,^{e,32} A.L. Lyon,⁴⁸ A.K.A. Maciel,² D. Mackin,⁷⁸ R. Madar,¹⁸ R. Magaña-Villalba,³² S. Malik,⁶⁴ V.L. Malyshev,³⁵ Y. Maravin,⁵⁷ J. Martínez-Ortega,³² R. McCarthy,⁷⁰ C.L. McGivern,⁵⁶ M.M. Meijer,³⁴ A. Melnitchouk,⁶³ D. Menezes,⁵⁰ P.G. Mercadante,⁴ M. Merkin,³⁷ A. Meyer,²¹ J. Meyer,²³ F. Miconi,¹⁹ N.K. Mondal,²⁹ G.S. Muanza,¹⁵ M. Mulhearn,⁷⁹ E. Nagy,¹⁵ M. Naimuddin,²⁸ M. Narain,⁷⁵ R. Nayyar,²⁸ H.A. Neal,⁶¹ J.P. Negret,⁸ P. Neustroev,³⁹ S.F. Novaes,⁵ T. Nunnemann,²⁵ G. Obrant,^{f,39} J. Orduna,⁷⁸ N. Osman,¹⁵ J. Osta,⁵⁴ G.J. Otero y Garzón,¹ M. Padilla,⁴⁶ A. Pal,⁷⁶ N. Parashar,⁵³ V. Parihar,⁷⁵ S.K. Park,³¹ J. Parsons,⁶⁸ R. Partridge,^{c,75} N. Parua,⁵² A. Patwa,⁷¹ B. Penning,⁴⁸ M. Perfilov,³⁷ K. Peters,⁴⁴ Y. Peters,⁴⁴ K. Petridis,⁴⁴ G. Petrillo,⁶⁹ P. Pétröff,¹⁶ R. Piegaia,¹ M.-A. Pleier,⁷¹ P.L.M. Podesta-Lerma,^{f,32} V.M. Podstavkov,⁴⁸ P. Polozov,³⁶ A.V. Popov,³⁸ M. Prewitt,⁷⁸ D. Price,⁵² N. Prokopenko,³⁸ S. Protopopescu,⁷¹ J. Qian,⁶¹ A. Quadt,²³ B. Quinn,⁶³ M.S. Rangel,² K. Ranjan,²⁸ P.N. Ratoff,⁴² I. Razumov,³⁸ P. Renkel,⁷⁷ M. Rijssenbeek,⁷⁰ I. Ripp-Baudot,¹⁹ F. Rizatdinova,⁷⁴ M. Rominsky,⁴⁸ A. Ross,⁴² C. Royon,¹⁸ P. Rubinov,⁴⁸ R. Ruchti,⁵⁴ G. Safronov,³⁶ G. Sajot,¹⁴ P. Salcido,⁵⁰ A. Sánchez-Hernández,³² M.P. Sanders,²⁵ B. Sanghi,⁴⁸ A.S. Santos,⁵ G. Savage,⁴⁸ L. Sawyer,⁵⁸ T. Scanlon,⁴³ R.D. Schamberger,⁷⁰ Y. Scheglov,³⁹ H. Schellman,⁵¹ T. Schliephake,²⁶ S. Schlobohm,⁸⁰ C. Schwanenberger,⁴⁴ R. Schwienhorst,⁶² J. Sekaric,⁵⁶ H. Severini,⁷³ E. Shabalina,²³ V. Shary,¹⁸ A.A. Shchukin,³⁸ R.K. Shivpuri,²⁸ V. Simak,¹⁰ V. Sirotenko,⁴⁸ P. Skubic,⁷³ P. Slattery,⁶⁹ D. Smirnov,⁵⁴ K.J. Smith,⁶⁷ G.R. Snow,⁶⁴ J. Snow,⁷² S. Snyder,⁷¹ S. Söldner-Rembold,⁴⁴ L. Sonnenschein,²¹ K. Soustruznik,⁹ J. Stark,¹⁴ V. Stolin,³⁶

D.A. Stoyanova,³⁸ M. Strauss,⁷³ D. Strom,⁴⁹ L. Stutte,⁴⁸ L. Suter,⁴⁴ P. Svoisky,⁷³ M. Takahashi,⁴⁴ A. Tanasijczuk,¹ W. Taylor,⁶ M. Titov,¹⁸ V.V. Tokmenin,³⁵ Y.-T. Tsai,⁶⁹ D. Tsybychev,⁷⁰ B. Tuchming,¹⁸ C. Tully,⁶⁶ L. Uvarov,³⁹ S. Uvarov,³⁹ S. Uzunyan,⁵⁰ R. Van Kooten,⁵² W.M. van Leeuwen,³³ N. Varelas,⁴⁹ E.W. Varnes,⁴⁵ I.A. Vasilyev,³⁸ P. Verdier,²⁰ L.S. Vertogradov,³⁵ M. Verzocchi,⁴⁸ M. Vesterinen,⁴⁴ D. Vilanova,¹⁸ P. Vokac,¹⁰ H.D. Wahl,⁴⁷ M.H.L.S. Wang,⁴⁸ J. Warchol,⁵⁴ G. Watts,⁸⁰ M. Wayne,⁵⁴ M. Weber^g,⁴⁸ L. Welty-Rieger,⁵¹ A. White,⁷⁶ D. Wicke,²⁶ M.R.J. Williams,⁴² G.W. Wilson,⁵⁶ M. Wobisch,⁵⁸ D.R. Wood,⁶⁰ T.R. Wyatt,⁴⁴ Y. Xie,⁴⁸ C. Xu,⁶¹ S. Yacoob,⁵¹ R. Yamada,⁴⁸ W.-C. Yang,⁴⁴ T. Yasuda,⁴⁸ Y.A. Yatsunenko,³⁵ Z. Ye,⁴⁸ H. Yin,⁴⁸ K. Yip,⁷¹ S.W. Youn,⁴⁸ J. Yu,⁷⁶ S. Zelitch,⁷⁹ T. Zhao,⁸⁰ B. Zhou,⁶¹ J. Zhu,⁶¹ M. Zielinski,⁶⁹ D. Ziemska,⁵² and L. Zivkovic⁷⁵

(The D0 Collaboration*)

¹Universidad de Buenos Aires, Buenos Aires, Argentina

²LAFEX, Centro Brasileiro de Pesquisas Físicas, Rio de Janeiro, Brazil

³Universidade do Estado do Rio de Janeiro, Rio de Janeiro, Brazil

⁴Universidade Federal do ABC, Santo André, Brazil

⁵Instituto de Física Teórica, Universidade Estadual Paulista, São Paulo, Brazil

⁶Simon Fraser University, Vancouver, British Columbia, and York University, Toronto, Ontario, Canada

⁷University of Science and Technology of China, Hefei, People's Republic of China

⁸Universidad de los Andes, Bogotá, Colombia

⁹Charles University, Faculty of Mathematics and Physics,
Center for Particle Physics, Prague, Czech Republic

¹⁰Czech Technical University in Prague, Prague, Czech Republic

¹¹Center for Particle Physics, Institute of Physics,

Academy of Sciences of the Czech Republic, Prague, Czech Republic

¹²Universidad San Francisco de Quito, Quito, Ecuador

¹³LPC, Université Blaise Pascal, CNRS/IN2P3, Clermont, France

¹⁴LPSC, Université Joseph Fourier Grenoble 1, CNRS/IN2P3,
Institut National Polytechnique de Grenoble, Grenoble, France

¹⁵CPPM, Aix-Marseille Université, CNRS/IN2P3, Marseille, France

¹⁶LAL, Université Paris-Sud, CNRS/IN2P3, Orsay, France

¹⁷LPNHE, Universités Paris VI and VII, CNRS/IN2P3, Paris, France

¹⁸CEA, Irfu, SPP, Saclay, France

¹⁹IPHC, Université de Strasbourg, CNRS/IN2P3, Strasbourg, France

²⁰IPNL, Université Lyon 1, CNRS/IN2P3, Villeurbanne, France and Université de Lyon, Lyon, France

²¹III. Physikalisches Institut A, RWTH Aachen University, Aachen, Germany

²²Physikalisches Institut, Universität Freiburg, Freiburg, Germany

²³II. Physikalisches Institut, Georg-August-Universität Göttingen, Göttingen, Germany

²⁴Institut für Physik, Universität Mainz, Mainz, Germany

²⁵Ludwig-Maximilians-Universität München, München, Germany

²⁶Fachbereich Physik, Bergische Universität Wuppertal, Wuppertal, Germany

²⁷Panjab University, Chandigarh, India

²⁸Delhi University, Delhi, India

²⁹Tata Institute of Fundamental Research, Mumbai, India

³⁰University College Dublin, Dublin, Ireland

³¹Korea Detector Laboratory, Korea University, Seoul, Korea

³²CINVESTAV, Mexico City, Mexico

³³Nikhef, Science Park, Amsterdam, the Netherlands

³⁴Radboud University Nijmegen, Nijmegen, the Netherlands and Nikhef, Science Park, Amsterdam, the Netherlands

³⁵Joint Institute for Nuclear Research, Dubna, Russia

³⁶Institute for Theoretical and Experimental Physics, Moscow, Russia

³⁷Moscow State University, Moscow, Russia

³⁸Institute for High Energy Physics, Protvino, Russia

³⁹Petersburg Nuclear Physics Institute, St. Petersburg, Russia

⁴⁰Institució Catalana de Recerca i Estudis Avançats (ICREA) and Institut de Física d'Altes Energies (IFAE), Barcelona, Spain

⁴¹Stockholm University, Stockholm and Uppsala University, Uppsala, Sweden

⁴²Lancaster University, Lancaster LA1 4YB, United Kingdom

⁴³Imperial College London, London SW7 2AZ, United Kingdom

⁴⁴The University of Manchester, Manchester M13 9PL, United Kingdom

⁴⁵University of Arizona, Tucson, Arizona 85721, USA

⁴⁶University of California Riverside, Riverside, California 92521, USA

⁴⁷Florida State University, Tallahassee, Florida 32306, USA

⁴⁸Fermi National Accelerator Laboratory, Batavia, Illinois 60510, USA

⁴⁹University of Illinois at Chicago, Chicago, Illinois 60607, USA

- ⁵⁰*Northern Illinois University, DeKalb, Illinois 60115, USA*
⁵¹*Northwestern University, Evanston, Illinois 60208, USA*
⁵²*Indiana University, Bloomington, Indiana 47405, USA*
⁵³*Purdue University Calumet, Hammond, Indiana 46323, USA*
⁵⁴*University of Notre Dame, Notre Dame, Indiana 46556, USA*
⁵⁵*Iowa State University, Ames, Iowa 50011, USA*
⁵⁶*University of Kansas, Lawrence, Kansas 66045, USA*
⁵⁷*Kansas State University, Manhattan, Kansas 66506, USA*
⁵⁸*Louisiana Tech University, Ruston, Louisiana 71272, USA*
⁵⁹*Boston University, Boston, Massachusetts 02215, USA*
⁶⁰*Northeastern University, Boston, Massachusetts 02115, USA*
⁶¹*University of Michigan, Ann Arbor, Michigan 48109, USA*
⁶²*Michigan State University, East Lansing, Michigan 48824, USA*
⁶³*University of Mississippi, University, Mississippi 38677, USA*
⁶⁴*University of Nebraska, Lincoln, Nebraska 68588, USA*
⁶⁵*Rutgers University, Piscataway, New Jersey 08855, USA*
⁶⁶*Princeton University, Princeton, New Jersey 08544, USA*
⁶⁷*State University of New York, Buffalo, New York 14260, USA*
⁶⁸*Columbia University, New York, New York 10027, USA*
⁶⁹*University of Rochester, Rochester, New York 14627, USA*
⁷⁰*State University of New York, Stony Brook, New York 11794, USA*
⁷¹*Brookhaven National Laboratory, Upton, New York 11973, USA*
⁷²*Langston University, Langston, Oklahoma 73050, USA*
⁷³*University of Oklahoma, Norman, Oklahoma 73019, USA*
⁷⁴*Oklahoma State University, Stillwater, Oklahoma 74078, USA*
⁷⁵*Brown University, Providence, Rhode Island 02912, USA*
⁷⁶*University of Texas, Arlington, Texas 76019, USA*
⁷⁷*Southern Methodist University, Dallas, Texas 75275, USA*
⁷⁸*Rice University, Houston, Texas 77005, USA*
⁷⁹*University of Virginia, Charlottesville, Virginia 22901, USA*
⁸⁰*University of Washington, Seattle, Washington 98195, USA*

We present a study of the dijet invariant mass spectrum in events with two jets produced in association with a W boson in data corresponding to an integrated luminosity of 4.3 fb^{-1} collected with the D0 detector at $\sqrt{s} = 1.96 \text{ TeV}$. We find no evidence for anomalous resonant dijet production and derive upper limits on the production cross section of an anomalous dijet resonance recently reported by the CDF Collaboration, investigating the range of dijet invariant mass from 110 to $170 \text{ GeV}/c^2$. The probability of the D0 data being consistent with the presence of a dijet resonance with 4 pb production cross section at $145 \text{ GeV}/c^2$ is 8×10^{-6} .

PACS numbers: 12.15.Ji, 12.38.Qk, 13.85.Rm, 14.80.-j

The CDF Collaboration at the Fermilab Tevatron $p\bar{p}$ collider recently reported a study of the dijet invariant mass (M_{jj}) spectrum in associated production with $W \rightarrow \ell\nu$ ($\ell = e$ or μ) at $\sqrt{s} = 1.96 \text{ TeV}$ with an integrated luminosity of 4.3 fb^{-1} [1]. In that paper they present evidence for an excess of events corresponding to 3.2 standard deviations (s.d.) above the background expectation, centered at $M_{jj} = 144 \pm 5 \text{ GeV}/c^2$ [1]. The CDF authors model this excess using a Gaussian peak with a width corresponding to an expected experimental M_{jj} resolution for the CDF detector [2] of $14.3 \text{ GeV}/c^2$

and further estimate the acceptance and selection efficiencies by simulating associated $W +$ Higgs boson (H) production in the decay mode $H \rightarrow b\bar{b}$ and with a mass $M_H = 150 \text{ GeV}/c^2$. Assuming the excess is caused by a particle X with $\mathcal{B}(X \rightarrow jj) = 1$, the CDF Collaboration reports an estimated production cross section of $\sigma(p\bar{p} \rightarrow WX) \approx 4 \text{ pb}$.

Using 5.3 fb^{-1} of integrated luminosity, the D0 Collaboration has previously set limits on resonant $b\bar{b}$ production in association with a W boson in dedicated searches for standard model (SM) Higgs bosons in the $WH \rightarrow \ell\nu b\bar{b}$ channel [3]. The D0 Collaboration reported upper limits on $\sigma(p\bar{p} \rightarrow WH) \times \mathcal{B}(H \rightarrow b\bar{b})$ ranging from approximately 0.62 pb for $M_H = 100 \text{ GeV}/c^2$ to 0.33 pb for $M_H = 150 \text{ GeV}/c^2$. The CDF Collaboration has performed a similar search using 2.7 fb^{-1} of integrated luminosity and reported no excess of events [4]. Furthermore, the D0 Collaboration has not observed a

^awith visitors from ^aAugustana College, Sioux Falls, SD, USA,

^bThe University of Liverpool, Liverpool, UK, ^cSLAC, Menlo Park, CA, USA,

^dUniversity College London, London, UK, ^eCentro de Investigacion en Computacion - IPN, Mexico City, Mexico,

^fECFM, Universidad Autonoma de Sinaloa, Culiacán, Mexico, and

^gUniversität Bern, Bern, Switzerland. [†]Deceased.

significant excess of associated W boson and dijet production in analyses of either $WW/WZ \rightarrow \ell\nu jj$ [5] or $H \rightarrow WW \rightarrow \ell\nu jj$ [6] using 1.1 fb^{-1} and 5.4 fb^{-1} of integrated luminosity, respectively.

In this Letter we report a study of associated $W(\rightarrow \ell\nu)$ and dijet production using data corresponding to 4.3 fb^{-1} of integrated luminosity collected with the D0 detector [7] at $\sqrt{s} = 1.96 \text{ TeV}$ at the Fermilab Tevatron $p\bar{p}$ Collider. The CDF study of this production process uses the same integrated luminosity. We investigate the dijet invariant mass range from 110 to $170 \text{ GeV}/c^2$ for evidence of anomalous dijet production.

To select $W(\rightarrow \ell\nu) + jj$ candidate events, we impose similar selection criteria to those used in the CDF analysis: a single reconstructed lepton (electron or muon) with transverse momentum $p_T > 20 \text{ GeV}/c$ and pseudorapidity [8] $|\eta| < 1.0$; missing transverse energy $\cancel{E}_T > 25 \text{ GeV}$; two jets reconstructed using a jet cone algorithm [9] with a cone of radius $\Delta R = 0.5$ that satisfy $p_T > 30 \text{ GeV}/c$ and $|\eta| < 2.5$, while vetoing events with additional jets with $p_T > 30 \text{ GeV}/c$. The separation between the two jets must be $|\Delta\eta(\text{jet}_1, \text{jet}_2)| < 2.5$, and the azimuthal separation between the most energetic jet and the direction of the \cancel{E}_T must satisfy $\Delta\phi(\text{jet}, \cancel{E}_T) > 0.4$. The transverse momentum of the dijet system is required to be $p_T(jj) > 40 \text{ GeV}/c$. To reduce the background from processes that do not contain $W \rightarrow \ell\nu$ decays, we require a transverse mass [10] of $M_T^{\ell\nu} > 30 \text{ GeV}/c^2$. In addition, we restrict $M_T^{\mu\nu} < 200 \text{ GeV}/c^2$ to suppress muon candidates with poorly measured momenta. Candidate events in the electron channel are required to satisfy a single electron trigger or a trigger requiring electrons and jets, which results in a combined trigger efficiency for the $e\nu jj$ selection of $(98^{+2}_{-3})\%$. A suite of triggers in the muon channel achieves a trigger efficiency of $(95 \pm 5)\%$ for the $\mu\nu jj$ selection. Lepton candidates must be spatially matched to a track that originates from the $p\bar{p}$ interaction vertex and they must be isolated from other energy depositions in the calorimeter and other tracks in the central tracking detector.

Most background processes are modeled using Monte Carlo (MC) simulation as in the CDF analysis. Diboson contributions (WW , WZ , ZZ) are generated with PYTHIA [11] using CTEQ6L1 parton distribution functions (PDF) [12]. The fixed-order matrix element (FOME) generator ALPGEN [13] with CTEQ6L1 PDF is used to generate $W+\text{jets}$, $Z+\text{jets}$, and $t\bar{t}$ events. The FOME generator COMPHEP [14] is used to produce single top-quark MC samples with CTEQ6M PDF. Both ALPGEN and COMPHEP are interfaced to PYTHIA for subsequent parton showering and hadronization. The MC events undergo a GEANT-based [15] detector simulation and are reconstructed using the same algorithms as used for D0 data. The effect of multiple $p\bar{p}$ interactions is included by overlaying data events from random beam crossings on simulated events. All MC samples except the

$W+\text{jets}$ are normalized to next-to-leading order (NLO) or next-to-NLO (NNLO) predictions for SM cross sections; the $t\bar{t}$, single t , and diboson cross sections are taken from Ref. [16], Ref. [17], and the MCFM program [18], respectively. The $Z+\text{jets}$ sample is normalized to the NNLO cross section [19]. The multijet background, in which a jet misidentified as an isolated lepton passes all selection requirements, is determined from data. In the muon channel, the multijet background is modeled with data events that fail the muon isolation requirements, but pass all other selections. In the electron channel, the multijet background is estimated using a data sample containing events that pass loosened electron quality requirements, but fail the tight electron quality criteria. All multijet samples are corrected for contributions from processes modeled by MC. The multijet normalizations in the two lepton channels are determined from fits to the $M_T^{\ell\nu}$ distributions, in which the multijet and $W+\text{jets}$ relative normalizations are allowed to float. The expected rate of multijet background is determined by this normalization, with an assigned uncertainty of 20%.

Corrections are applied to the MC to account for differences from data in reconstruction and identification efficiencies of leptons and jets. Also, trigger efficiencies measured in data are applied to MC. The instantaneous luminosity profile and z position of the $p\bar{p}$ interaction vertex of each MC sample are adjusted to match those in data. The p_T distribution of Z bosons is corrected at the generator level to reproduce dedicated measurements [20].

Other D0 analyses of this final state apply additional corrections to improve the modeling of the $W+\text{jets}$ and $Z+\text{jets}$ production in the MC [3]. For the results presented in this Letter, we choose not to apply those corrections in order to parallel the CDF analysis. We did, however, study the effects of applying such corrections [21] and find they do not alter our conclusions.

We consider the effect of systematic uncertainties on both the normalization and the shape of dijet invariant mass distributions. Systematic effects are considered from a range of sources: the choice of renormalization and factorization scales, the ALPGEN parton-jet matching algorithm [22], jet energy resolution, jet energy scale, and modeling of the underlying event and parton showering. Uncertainties on the choice of PDF, as well as uncertainties from object reconstruction and identification, are evaluated for all MC samples.

In Fig. 1 we present the dijet invariant mass distribution after a fit of the sum of SM contributions to data. Other distributions are available in the supplementary material [21]. The fit minimizes a Poisson χ^2 -function with respect to variations in the rates of individual background sources and systematic uncertainties that may modify the predicted dijet invariant mass distribution [23]. A Gaussian prior is used for each systematic uncertainty, including those on the normalization of each

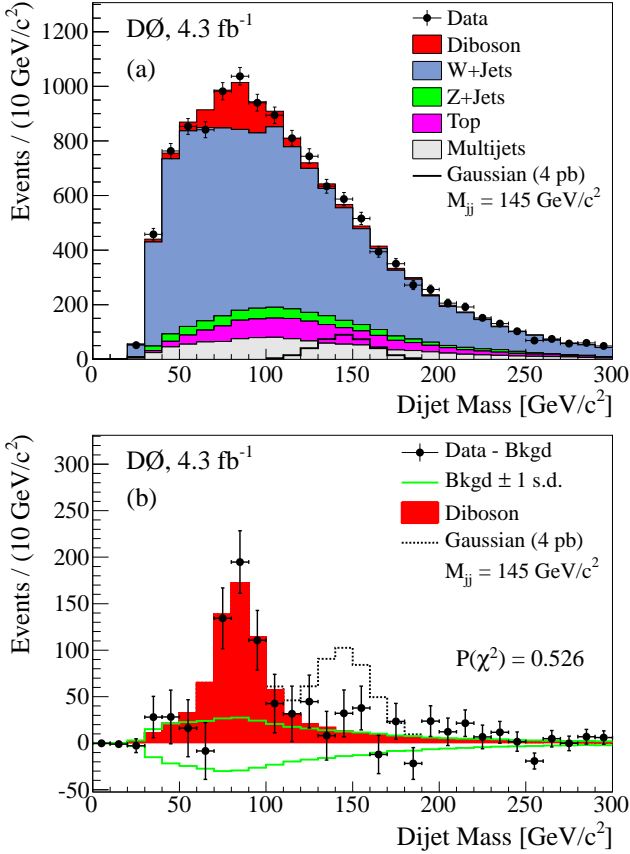


FIG. 1: (color online) Dijet invariant mass summed over electron and muon channels after the fit without (a) and with (b) subtraction of SM contributions other than that from the SM diboson processes, along with the ± 1 s.d. systematic uncertainty on all SM predictions. The χ^2 fit probability, $P(\chi^2)$, is based on the residuals using data and MC statistical uncertainties. Also shown is the relative size and shape for a model with a Gaussian resonance with a production cross section of 4 pb at $M_{jj} = 145 \text{ GeV}/c^2$.

sample, but the cross sections for diboson and W -jets production in the MC are floated with no constraint. The fit computes the optimal values of the systematic uncertainties, accounting for departures from the nominal predictions by including a term in the fit function that sums the squared deviation of each systematic in units normalized by its ± 1 s.d. Different uncertainties are assumed to be mutually independent, but those common to both lepton channels are treated as fully correlated. We perform fits to electron and muon selections simultaneously and then sum them to obtain the dijet invariant mass distributions shown in Fig. 1. The measured yields after the fit are given in Table I.

To probe for an excess similar to that observed by the CDF Collaboration [1], we model a possible signal as a Gaussian resonance in the dijet invariant mass with an observed width corresponding to the expected resolution of the D0 detector given by $\sigma_{jj} = \sigma_{W \rightarrow jj} \cdot \sqrt{M_{jj}/M_{W \rightarrow jj}}$.

TABLE I: Yields determined following a χ^2 fit to the data, as shown in Fig. 1. The total uncertainty includes the effect of correlations between the individual contributions as determined using the covariance matrix.

	Electron channel	Muon channel
Dibosons	434 ± 38	304 ± 25
W +jets	5620 ± 500	3850 ± 290
Z +jets	180 ± 42	350 ± 60
$t\bar{t}$ + single top	600 ± 69	363 ± 39
Multijet	932 ± 230	151 ± 69
Total predicted	7770 ± 170	5020 ± 130
Data	7763	5026

Here, $\sigma_{W \rightarrow jj}$ and $M_{W \rightarrow jj}$ are the width and mass of the $W \rightarrow jj$ resonance, determined to be $\sigma_{W \rightarrow jj} = 11.7 \text{ GeV}/c^2$ and $M_{W \rightarrow jj} = 81 \text{ GeV}/c^2$ from a simulation of $WW \rightarrow \ell\nu jj$ production. For a dijet invariant mass resonance at $M_{jj} = 145 \text{ GeV}/c^2$, the expected width is $\sigma_{jj} = 15.7 \text{ GeV}/c^2$.

We normalize the Gaussian model in the same way as reported in the CDF Letter [1]. We assume that any such excess comes from a particle X that decays to jets with 100% branching fraction. The acceptance for this hypothetical process ($WX \rightarrow \ell\nu jj$) is estimated from a MC simulation of $WH \rightarrow \ell\nu b\bar{b}$ production. When testing the Gaussian signal with a mean of $M_{jj} = 145 \text{ GeV}/c^2$, the acceptance is taken from the $WH \rightarrow \ell\nu b\bar{b}$ simulation with $M_H = 150 \text{ GeV}/c^2$. This prescription is chosen to be consistent with the CDF analysis, which used a simulation of $WH \rightarrow \ell\nu b\bar{b}$ production with $M_H = 150 \text{ GeV}/c^2$ to estimate the acceptance for the excess that they observe at $M_{jj} = 144 \text{ GeV}/c^2$. When probing other values of M_{jj} , we use the acceptance obtained for $WH \rightarrow \ell\nu b\bar{b}$ MC events with $M_H = M_{jj} + 5 \text{ GeV}/c^2$.

We use this Gaussian model to derive upper limits on the cross section for a possible dijet resonance as a function of dijet invariant mass using the CL_s method with a negative log-likelihood ratio (LLR) test statistic [24] that is summed over all bins in the dijet invariant mass spectrum. Upper limits on cross section are calculated at the 95% confidence level (C.L.) for Gaussian signals with mean dijet invariant mass in the range $110 < M_{jj} < 170 \text{ GeV}/c^2$, in steps of $5 \text{ GeV}/c^2$, allowing the cross sections for W -jets production to float with no constraint. Other contributions are constrained by the *a priori* uncertainties on their rate, either derived from theory or subsidiary measurements.

The Gaussian model is assigned systematic uncertainties affecting both the normalization and shape of the distribution derived from the systematic uncertainties on the diboson simulation. A fit [23] of both the signal+background and background-only hypotheses is performed for an ensemble of pseudo-experiments as well as for the data distribution. The results of the cross section upper limit calculation are shown in Fig. 2 and are

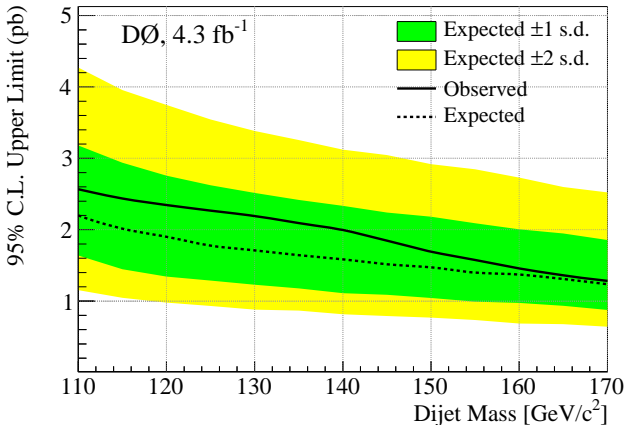


FIG. 2: (color online) Upper limits on the cross section (in pb) at the 95% C.L. for a Gaussian signal in dijet invariant mass. Shown are the limit expected using the background prediction, the observed data, and the regions corresponding to a 1 s.d. and 2 s.d. fluctuation of the backgrounds.

summarized in Table II.

In a further effort to evaluate the sensitivity for any excess of events of the type reported by the CDF Collaboration, we perform a signal-injection test. We repeat the statistical analysis after injecting a Gaussian signal model, normalized to a cross section of 4 pb, into the D0 data sample, thereby creating a mock “data” sample modeling the expected outcome with a signal present. The size and shape of the injected Gaussian model for $M_{jj} = 145 \text{ GeV}/c^2$ relative to other data components is shown in Fig. 1.

The LLR metric provides a sensitive measure of model compatibility, providing information on both the rate and mass of any signal-like excess. We therefore study the LLR distributions obtained with actual data as well as the signal-injected mock data sample. The results of the LLR test in Fig. 3 show a striking difference between the two hypotheses, demonstrating that this analysis is sensitive to the purported excess. In the actual data, however, no significant evidence for an excess is observed.

In Fig. 4, we show as a function of cross section the p -value obtained by integrating the LLR distribution populated from pseudo-experiments drawn from the signal+background hypothesis above the observed LLR, assuming a Gaussian invariant mass distribution with a mean of $M_{jj} = 145 \text{ GeV}/c^2$. The p -value for a Gaussian signal with cross section of 4 pb is 8.0×10^{-6} , corresponding to a rejection of this signal cross section at a Gaussian equivalent of 4.3 s.d. We set a 95% C.L. upper limit of 1.9 pb on the production cross section of such a resonance.

In summary, we have used 4.3 fb^{-1} of integrated luminosity collected with the D0 detector to study the dijet invariant mass spectrum in events containing one $W \rightarrow \ell\nu$ ($\ell = e$ or μ) boson decay and two high- p_T

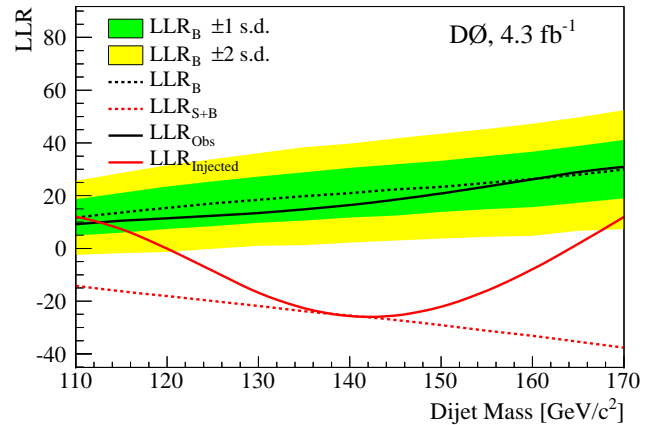


FIG. 3: (color online) Log-likelihood ratio test statistic as a function of probed dijet mass. Shown are the expected LLR for the background prediction (dashed black) with regions corresponding to a 1 s.d. and 2 s.d. fluctuation of the backgrounds, for the signal+background prediction (dashed red), for the observed data (solid black), and for data with a dijet invariant mass resonance at $145 \text{ GeV}/c^2$ injected with a cross section of 4 pb (solid red).

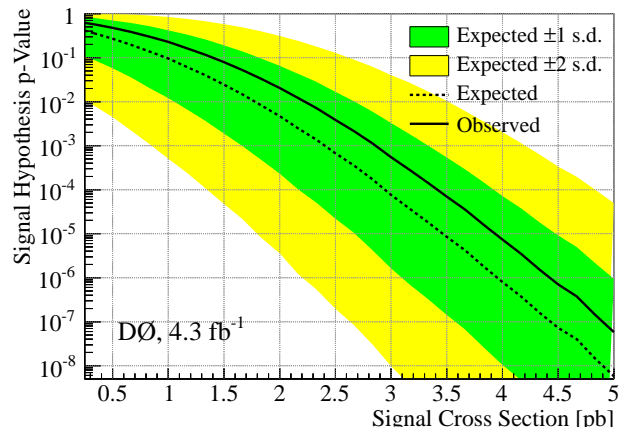


FIG. 4: (color online) Distribution of p -values for the signal+background hypothesis with a Gaussian signal with mean of $M_{jj} = 145 \text{ GeV}/c^2$ as a function of hypothetical signal cross section (in pb). Shown are the p -values for the background prediction (dashed black) with regions corresponding to a 1 s.d. and 2 s.d. fluctuation of the backgrounds and the observed data (solid black).

jets. Utilizing a similar data selection as the CDF Collaboration we find no evidence for anomalous, resonant production of dijets in the mass range $110 - 170 \text{ GeV}/c^2$. Using a simulation of $WH \rightarrow \ell\nu b\bar{b}$ production to model acceptance and efficiency, we derive upper limits on the cross section for anomalous resonant dijet production. For $M_{jj} = 145 \text{ GeV}/c^2$, we set a 95% C.L. upper limit of 1.9 pb on the cross section and we reject the hypothesis of a production cross section of 4 pb at the level of 4.3 s.d.

We thank the staffs at Fermilab and collaborating

TABLE II: Expected and observed upper limits on the cross section (in pb) at the 95% C.L. for a dijet invariant mass resonance.

M_{jj} (GeV)	110	115	120	125	130	135	140	145	150	155	160	165	170
Expected:	2.20	2.01	1.90	1.78	1.71	1.64	1.58	1.52	1.47	1.40	1.37	1.31	1.24
Observed:	2.57	2.44	2.35	2.27	2.19	2.09	2.00	1.85	1.69	1.58	1.46	1.36	1.28

institutions, and acknowledge support from the DOE and NSF (USA); CEA and CNRS/IN2P3 (France); FASI, Rosatom and RFBR (Russia); CNPq, FAPERJ, FAPESP and FUNDUNESP (Brazil); DAE and DST (India); Colciencias (Colombia); CONACyT (Mexico); KRF and KOSEF (Korea); CONICET and UBACyT (Argentina); FOM (The Netherlands); STFC and the Royal Society (United Kingdom); MSMT and GACR (Czech Republic); CRC Program and NSERC (Canada); BMBF and DFG (Germany); SFI (Ireland); The Swedish Research Council (Sweden); and CAS and CNSF (China).

running along the proton beam axis. The angles θ and ϕ are the polar and azimuthal angles, respectively. Pseudorapidity is defined as $\eta = -\ln [\tan(\theta/2)]$, in which θ is measured with respect to the proton beam direction.

- [9] G. C. Blazey *et al.*, arXiv:hep-ex/0005012 (2000). The seeded iterative mid-point cone algorithm with radius $\Delta R = \sqrt{(\Delta\phi)^2 + (\Delta\eta)^2} = 0.5$ was used.
- [10] J. Smith, W. L. van Neerven, and J. A. M. Vermaseren, Phys. Rev. Lett. **50**, 1738 (1983).
- [11] T. Sjöstrand, S. Mrenna, and P. Skands, J. High Energy Phys. **05**, 026 (2006). Version 6.3 was used.
- [12] J. Pumplin *et al.*, J. High Energy Phys. **07**, 012 (2002); D. Stump *et al.*, J. High Energy Phys. **10**, 046 (2003).
- [13] M. L. Mangano *et al.*, J. High Energy Phys. **07**, 001 (2003). Version 2.05 was used.
- [14] A. Pukhov *et al.*, arXiv:hep-ph/9908288 (2000).
- [15] R. Brun, F. Carminati, CERN Program Library Long Writeup W5013 (1993).
- [16] N. Kidonakis and R. Vogt, Phys. Rev. D **78**, 074005 (2008).
- [17] N. Kidonakis, Phys. Rev. D **74**, 114012 (2006).
- [18] J. M. Campbell and R. K. Ellis, Phys. Rev. D **60**, 113006 (1999).
- [19] R. Hamberg, W. L. van Neerven, and W. B. Kilgore, Nucl. Phys. B **359**, 343 (1991); **644**, 403(E) (2002).
- [20] V. M. Abazov *et al.*, Phys. Rev. Lett. **100**, 102002 (2008).
- [21] See EPAPS Document No. E-PRL for additional material. For more information on EPAPS, see <http://www.aip.org/pubservs/epaps.html>.
- [22] S. Höche *et al.*, arXiv:hep-ph/0602031 (2006).
- [23] W. Fisher, FERMILAB-TM-2386-E (2006).
- [24] T. Junk, Nucl. Instrum. Meth. A **434**, 435 (1999); A. Read, J. Phys. G **28**, 2693 (2002).

-
- [1] T. Aaltonen *et al.* (CDF Collaboration), Phys. Rev. Lett. **106**, 171801 (2011).
 - [2] D. Acosta *et al.* (CDF Collaboration), Phys. Rev. D **71**, 032001 (2005).
 - [3] V. M. Abazov *et al.* (D0 Collaboration), Phys. Lett. B **698**, 6 (2011).
 - [4] T. Aaltonen *et al.* (CDF Collaboration), Phys. Rev. Lett. **103**, 101802 (2009).
 - [5] V. M. Abazov *et al.* (D0 Collaboration), Phys. Rev. Lett. **102**, 161801 (2009).
 - [6] V. M. Abazov *et al.* (D0 Collaboration), Phys. Rev. Lett. **106**, 171802 (2011).
 - [7] B. Abbott *et al.* (D0 Collaboration), Nucl. Instrum. Methods Phys. Res. A **565**, 463 (2006); M. Abolins *et al.*, Nucl. Instrum. and Methods A **584**, 75 (2007); R. Angstadt *et al.*, Nucl. Instrum. Methods Phys. Res. A **622**, 298 (2010).
 - [8] D0 uses a spherical coordinate system with the z axis